CDDpress

www.nature.com/cddiscovery

ARTICLE OPEN

Check for updates

EIF4EBP1 is transcriptionally upregulated by MYCN and associates with poor prognosis in neuroblastoma

Kai Voeltzke[1], Katerina Scharov[1,2], Cornelius Maximilian Funk[3,4,5], Alisa Kahler[1], Daniel Picard[1,2,6], Laura Hauffe[1], Martin F. Orth[3], Marc Remke[1,2,6], Irene Esposito[7], Thomas Kirchner[8,9], Alexander Schramm[10], Barak Rotblat[11,12], Thomas G. P. Grünewald[3,4,5,13], Guido Reifenberger[1,6] and Gabriel Leprivier[1]✉

Neuroblastoma (NB) accounts for 15% of cancer-related deaths in childhood despite considerable therapeutic improvements. While several risk factors, including *MYCN* amplification and alterations in RAS and p53 pathway genes, have been defined in NB, the clinical outcome is very variable and difficult to predict. Since genes of the mechanistic target of rapamycin (mTOR) pathway are upregulated in *MYCN*-amplified NB, we aimed to define the predictive value of the mTOR substrate-encoding gene eukaryotic translation initiation factor 4E-binding protein 1 (*EIF4EBP1*) expression in NB patients. Using publicly available data sets, we found that *EIF4EBP1* mRNA expression is positively correlated with *MYCN* expression and elevated in stage 4 and high-risk NB patients. In addition, high *EIF4EBP1* mRNA expression is associated with reduced overall and event-free survival in the entire group of NB patients in three cohorts, as well as in stage 4 and high-risk patients. This was confirmed by monitoring the clinical value of 4EBP1 protein expression, which revealed that high levels of 4EBP1 are significantly associated with prognostically unfavorable NB histology. Finally, functional analyses revealed that *EIF4EBP1* expression is transcriptionally controlled by MYCN binding to the *EIF4EBP1* promoter in NB cells. Our data highlight that *EIF4EBP1* is a direct transcriptional target of MYCN whose high expression is associated with poor prognosis in NB patients. Therefore, *EIF4EBP1* may serve to better stratify patients with NB.

Cell Death Discovery (2022)8:157 ; https://doi.org/10.1038/s41420-022-00963-0

INTRODUCTION

Neuroblastoma (NB) is a pediatric malignant tumor that develops from progenitor cells of the sympathetic nervous system and the adrenal glands [1, 2]. NB is the most commonly occurring extracranial solid tumor in childhood and the major cause of cancer-related mortality in infants [2]. NB tumors are classified into five stages (1, 2, 3, 4, and 4S) according to tumor size, the presence of metastasis, and the outcome of surgical resection [1]. Noteworthy, stage 4S represents a special form of NB in infants that is associated with a high chance of spontaneous regression despite metastatic spread [1]. Apart from surgical resection, treatment options may include response-adjusted chemotherapy for low to intermediate risk groups or a mix of surgery, high-dose chemotherapy, immunotherapy, and radiation for patients belonging to the high-risk group. The risk level is determined based on the tumor stage combined with age at diagnosis, tumor ploidy, genetic alterations, and tumor histology [1, 3]. However, NB represents a particularly heterogeneous type of cancer, posing challenges to precisely predict therapeutic response and clinical outcome in the individual patient [4, 5]. While some NB tumors may spontaneously regress, high-risk patients have an increased likelihood of relapse and available treatment options for relapsed patients are rarely successful. Indeed, the 5-year overall survival rate for high-risk patients is ranging from 31 to 86%, in contrast to 97–100% for low-risk patients [6]. In addition, success rates of second line treatment in relapsed patients remain poor [5, 7]. Therefore, it is critical to define novel stratification factors for NB patients to better predict individual risk and to facilitate administration of the most appropriate therapeutic option.

NB is rarely familial (1–2%) and only few predisposition genes, such as *PHOX2B* and *ALK*, have been reported [4, 8–10]. Genetically, several acquired alterations have been detected in NB and linked to patient outcome. These include gain-of-function mutations in *ALK*, gain of chromosome arm 17q, loss of chromosome arm 11q, amplification of *MYCN* [4, 11], and, more recently reported, alterations in genes related to the RAS and p53 pathways [12]. *MYCN* amplification is found in about 20% of NB and is associated with aggressive tumors, therapy resistance and poor survival [13]. *MYCN* is a member of the *MYC* oncogene family and encodes a transcription factor that recognizes a specific DNA

[1]Institute of Neuropathology, University Hospital Düsseldorf, Medical Faculty, Heinrich Heine University, Düsseldorf, Germany. [2]Department of Pediatric Oncology, Hematology, and Clinical Immunology, University Hospital Düsseldorf, Medical Faculty, Heinrich Heine University, Düsseldorf, Germany. [3]Faculty of Medicine, Max-Eder Research Group for Pediatric Sarcoma Biology, Institute of Pathology, LMU Munich, Munich, Germany. [4]Division of Translational Pediatric Sarcoma Research, German Cancer Research Center (DKFZ), Heidelberg, Germany. [5]Hopp Children's Cancer Center (KiTZ), Heidelberg, Germany. [6]German cancer consortium (DKTK), partner site Essen/Düsseldorf, Düsseldorf, Germany. [7]Institute of Pathology, Heinrich Heine University, Medical Faculty, and University Hospital Düsseldorf, Düsseldorf, Germany. [8]Institute of Pathology, Faculty of Medicine, LMU Munich, Munich, Germany. [9]German cancer consortium (DKTK) partner site Munich, Munich, Germany. [10]Department of Medical Oncology, West German Cancer Center, University of Duisburg-Essen, Essen, Germany. [11]Department of Life Sciences, Ben-Gurion University of the Negev, Beer Sheva, Israel. [12]The National Institute for Biotechnology in the Negev, Beer Sheva, Israel. [13]Institute of Pathology, Heidelberg University Hospital, Heidelberg, Germany. ✉email: gabriel.leprivier@med.uni-duesseldorf.de

Received: 19 January 2022 Revised: 10 March 2022 Accepted: 18 March 2022
Published online: 04 April 2022

element referred to as E-box [14, 15]. This allows MYCN to regulate the transcription of genes involved in cell cycle progression, proliferation, differentiation, and survival [13]. MYCN is a strong driver of NB tumorigenesis, as tissue-specific overexpression of MYCN is sufficient to induce NB tumor development in mouse models [16]. Mechanistically, MYCN is proposed to rewire metabolism to enable NB tumor cells to proliferate, in turn preserving the intracellular redox balance while producing enough energy by inducing a glycolytic switch [17–19]. In particular, MYCN actively augments the transcription of multiple genes whose products are involved in the protein synthesis machinery [18]. Even though MYCN represents a highly attractive therapeutic target in NB, as a transcription factor that lacks hydrophobic pockets which can be targeted by drug-like small molecules, it is still considered as being "undruggable" [20, 21]. Thus, identification of downstream effectors involved in MYCN-driven NB progression is a promising approach to uncover novel targets for molecularly guided therapeutic approaches.

To better delineate the molecular basis of *MYCN*-amplified NB aggressiveness, several approaches have been undertaken. In particular, RNA-sequencing (RNA-seq) has been used to uncover the set of genes induced in *MYCN*-amplified compared to *MYCN*-non-amplified NB [22]. Strikingly, this analysis identified regulators of protein synthesis which are components of the mechanistic target of rapamycin (mTOR) pathway, including the mTOR target eukaryotic initiation factor 4E binding protein 1 (*EIF4EBP1*). The corresponding protein, 4EBP1, is inhibited through mTOR-mediated phosphorylation when nutrients are available, leading to active mRNA translation initiation [23]. Under nutrient-deprived conditions, when mTOR is inhibited, 4EBP1 gets activated and thus binds to the translation initiation factor eIF4E, in turn blocking cap-dependent mRNA translation initiation [23]. At the cellular level, 4EBP1 is negatively regulating proliferation and mitochondrial activity [24, 25]. The exact role of 4EBP1 in cancer is still debated. 4EBP1 was found to exert a tumor suppressive function in vivo, as 4EBP1 knock-out leads to enhanced tumor formation in mouse models of head and neck squamous cell carcinoma [26], and prostate cancer [27]. In contrast, 4EBP1 was shown to mediate angiogenesis and facilitate tumor growth in a breast cancer model in vivo, highlighting a cancer type-specific function of 4EBP1 [28]. In keeping with that, the clinical relevance of *EIF4EBP1* expression depends on the tumor type. *EIF4EBP1* was reported to be overexpressed in a number of tumor entities in adults [29], including breast cancer [30], in which *EIF4EBP1* is amplified as part of the 8p11–12 amplicon, as well as in ovarian and prostate cancer [31, 32]. In breast and liver cancer, high *EIF4EBP1* expression has been associated with poor survival [30, 33]. In contrast, *EIF4EBP1* expression was found to be reduced in head and neck cancer, in which low expression is correlated with poor prognosis [26]. In NB, the expression of *EIF4EBP1* is deregulated, even though contradictory findings have been reported. While *EIF4EBP1* was characterized as a gene upregulated in *MYCN*-amplified versus *MYCN*-non-amplified NB tissues and cells [22], another study reported that *EIF4EBP1* levels were higher in favorable stages of NB as compared to advanced stage 4 tumors [34]. In addition, Meng *et al*. showed that *EIF4EBP1* is part of a gene signature that predicts poor overall survival [35]. However, it was not investigated whether *EIF4EBP1* expression alone can predict NB patient prognosis. Thus, the clinical relevance of *EIF4EBP1* expression in NB needs further evaluation. Overexpression of *EIF4EBP1* in cancer is mediated by certain transcription factors, such as MYC [36, 37], androgen receptor [38], and the stress regulators ATF4 [39] and HIF-1α [40], which all bind to and thereby modulate the activity of the *EIF4EBP1* promoter. More specifically, ChIP-sequencing (ChIP-seq) revealed binding of MYCN to the *EIF4EBP1* promoter in NB cells, and MYCN was reported to impact *EIF4EBP1* transcription, pointing to *EIF4EBP1* as a potential MYCN target gene [41, 42]. However, how MYCN exactly controls the *EIF4EBP1* promoter is still poorly understood.

In this study, we analyzed publicly available NB patient data sets and revealed that *EIF4EBP1* is overexpressed in NB compared to normal tissues, is significantly co-expressed with *MYCN*, and is elevated in high-risk relatively to low-risk tumor groups. High *EIF4EBP1* levels were found to be significantly linked to poor overall survival in all NB patients, as well as in the more aggressive stage 4 and high-risk groups. In addition, immunohistochemistry staining of NB tissues confirmed the mRNA-based associations and showed that high 4EBP1 protein expression associates with unfavorable histology in NB. Finally, by applying gene reporter assays and by modulating MYCN expression in vitro, we found that MYCN upregulates the *EIF4EBP1* promoter activity by binding to three distinct E-boxes.

MATERIALS AND METHODS

Databases

The RNA-seq, microarray, and ChIP-seq data were retrieved from 'R2: Genomics Analysis and Visualization Platform' (http://r2.amc.nl). Data were visualized with IGV or Affinity Designer. For the MYCN occupancy profile in BE(2)-C cells, the ChIP-seq data by Durbin et al. (GSE94824) were accessed using the human genome GRCh 38/hg 38. For the initial across dataset analysis, "Normal Adrenal gland" dataset from R2 (corresponding to samples taken from multiple data sets [GSE3526, GSE7307, GSE8514] and combined into a single data set) and four publicly available and independent cohorts, namely the Versteeg et al. (GSE16476), Lastowska et al. (GSE13136), Hiyama et al. (GSE16237), and Delattre et al. (GSE14880) datasets were used. The normalization was done automatically by R2 using MAS5.0. The remaining expression, amplification, and survival data consisted of the independent SEQC/ MAQC-III Consortium (GSE49710), Kocak et al. study (GSE45547) and Neuroblastoma Research Consortium [NRC] (GSE85047) cohorts. For the expression analysis of TH-MYCN transgenic NB model, the dataset from Balamuth et al. (GSE17740) was used. For the expression analysis of SH-SY5Y cells treated with all-trans retinoic acid (RA), the dataset from Takeda et al. (GSE9169) was used.

Immunohistochemistry

For immunohistochemistry, deparaffinated tissue sections were pretreated with citrate buffer at 98 °C for 20 min, cooled down to room temperature, and blocked with 2% horse serum, avidin blocking solution, and biotin blocking solution (Avidin/Biotin Blocking Kit, SP-2001, Vector Laboratories, Burlingame, CA, USA) for 10 min each. Staining for 4EBP1 was carried out with monoclonal anti-4EBP1 raised in rabbit (1:200; ab32024, Abcam, Cambridge, UK) for 2 h at 37 °C. Detection was carried out using the Dako REAL detection system, alkaline phosphatase/RED, rabbit/mouse following manufacturer´s instructions (Detection Kit #K5005, Agilent Technologies, Santa Clara, CA, USA). Immunostained tissue sections were counterstained with hematoxylin solution according to Mayer (T865.1, Roth, Karlsruhe, Germany).

Evaluation of immunoreactivity of 4EBP1 was carried out in analogy to scoring of hormone receptor Immune Reactive Score (IRS) ranging from 0–12. The percentage of cells with expression of the given antigen was scored and classified in five grades (grade 0 = 0–19%, grade 1 = 20–39%, grade 2 = 40–59%, grade 3 = 60–79%, and grade 4 = 80 − 100%). In addition, the intensity of marker immunoreactivity was determined (grade 0 = none, grade 1 = low, grade 2 = moderate and grade 3 = strong). The product of these two grades defined the final IRS. IRS 0–6 was considered as "low" staining level while IRS 7–12 was categorized as "high" staining level.

Tissue microarrays (TMAs) were constructed by taking three representative cores (each 1 mm in diameter) from respective blocks exhibiting at least 80% viable tumor tissue. Tumor blocks were retrieved from the archives of the Institutes of Pathology of the LMU Munich or the University Hospital Düsseldorf with IRB approval (study numbers 550-16 UE for LMU Munich and 2018-174 for the University Hospital Düsseldorf). Informed consent was obtained from all patients.

Statistics

All experiments were, if not otherwise stated, independently carried out at least three times. Statistical significance was calculated using Student's *t*

test or Mann–Whitney *U*-test in GraphPad Prism 8. For survival analysis, the cohorts were stratified based on relative expression of *EIF4EBP1*. The median was chosen as expression cutoff to determine high and low *EIF4EBP1* level. Statistical significance was determined by the logrank test. Multivariate analysis was performed using the Cox Regression method in SPSS v21 (IBM, Armonk, NY, USA). To calculate significance of the scoring of immunohistochemistry staining, the Chi-square test was used. The data are represented as means ± standard deviation. A p-value of less than 0.05 was considered significant.

Cell culture

Cells were maintained using standard tissue culture procedures in a humidified incubator at 37 °C with 5% CO_2 and atmospheric oxygen. NB cell lines IMR-32 and Kelly, and HEK-293-T cells were obtained from American Type Culture Collections (ATCC, Manassas, VA, USA). SHEP-TR-MYCN engineered NB cell lines have been previously described [19]. NB cell lines were cultured in Roswell Park Memorial Institute (RPMI)-1640 medium (Thermo Fisher Scientific, Waltham, MA, USA), while HEK-293-T cells were maintained in Dulbecco's modified Eagle medium (DMEM) (Thermo Fisher Scientific). All cell culture media were supplemented with 10% (volume/volume) fetal bovine serum (FBS) (Sigma-Aldrich, St. Louis, MI, USA) and 1% penicillin/streptomycin (Thermo Fisher Scientific). Cells were treated with 3 µg/ml plasmocin (Invivogen, San Diego, CA, USA) to prevent mycoplasma contamination. To induce MYCN expression, SHEP-TR-MYCN cells were treated with 1 µg/ml doxycycline. All cell lines were routinely confirmed to be mycoplasma-free using Venor®GeM Classic kit (Minerva Biolabs, Berlin, Germany). Cell lines were authenticated by STR-profiling (Genomics and Transcriptomics Laboratory, Heinrich Heine University, Dusseldorf, Germany).

RNA extraction, cDNA synthesis, and quantitative real-time PCR

Total RNA was purified from cells using the RNeasy plus mini kit (QIAgen, Hilden, Germany) according to the manufacturer's handbook. RNA concentration and purity were assessed by spectrophotometry using the NanoDrop2000 (Thermo Fisher Scientific). Subsequently, each sample was diluted to a concentration of 100 ng/µl in nuclease-free water. For cDNA synthesis, 1 µg RNA was processed in a total reaction volume of 20 µl using the High-Capacity cDNA Reverse Transcription kit (Applied Biosystems, Waltham, MA, USA), following the manufacturer's protocol. Quantitative real-time reverse transcription (qRT) PCR was performed using SYBR green PCR master mix (Applied Biosystems) and the CFX384 Touch Real-Time PCR Detection System (Bio-Rad Laboratories, Hercules, CA, USA). Relative expression levels of *MYCN* and *EIF4EBP1* were normalized to internal housekeeping genes *GUSB* and *PPIA*. The primer list can be found in supplementary table 1.

Immunoblot analysis of protein expression

Cells were washed with phosphate-buffered saline (PBS) and lysed in radioimmunoprecipitation assay (RIPA) buffer (150 mM NaCl, 50 mM Tris-HCl, pH 8, 1% Triton X-100, 0.5% sodium deoxycholate, and 0.1% SDS) supplemented with protease inhibitors (Sigma-Aldrich) and phosphatase inhibitors mix (PhosphoSTOP, Roche, Penzberg, Germany). Cell lysates were centrifuged at 21,000 rpm for 15 min at 4 °C to separate cell debris and DNA from protein lysates. Protein concentration was measured with the BCA protein assay kit (Thermo Fisher Scientific), according to manufacturer's protocol. Protein lysates were separated by SDS-PAGE and transferred onto a nylon membrane. The membrane was incubated for 1 h in Tris-buffered saline Tween (TBST) (50 mM Tris-Cl, 150 mM NaCl, pH 7.5, 0.1% Tween-20) containing 5% bovine serum albumin (BSA), to prevent non-specific antibody binding, followed by an overnight incubation at 4 °C with the following primary antibodies: 4EBP1 (1:1000; #9644, Cell Signaling Technology, Cambridge, UK), MYCN (1:1,000; #9405, Cell Signaling Technology), GAPDH (1:1000; #2118, Cell Signaling Technology), and β-Actin (1:5,000; #A2228, Sigma-Aldrich). The secondary antibodies IRDye 800CW Goat anti-Rabbit (1:10,000; #926-32211, LI-COR Biosciences, Bad Homburg, Germany) or IRDye 800CW Goat anti-Mouse (1:10,000; #926-32210, LI-COR Biosciences) were incubated at room temperature for 1 h, followed by detection of the fluorescent signal with the Odyssey CLx imager (LI-COR Biosciences).

Plasmid construction

The promoter region of the human *EIF4EBP1* gene, spanning from −192 to +1372, was inserted into the SacI and BglII restriction sites of the firefly luciferase expressing pGL4.22 plasmid (Promega, Madison, WI, USA). Each of the three identified MYCN binding site was subsequently mutated alone or in a combination of two sites. Each of the E-box sequence has been mutated to CAAGGC. All cloning was performed by GENEWIZ Germany GmbH (Leipzig, Germany).

Luciferase Reporter Assay

For the promoter reporter assay, HEK-293-T cells were seeded into 12-well plates and co-transfected the following day with 500 ng of the *EIF4EBP1* WT or mutant promoter pGL4.22 plasmids, 50 ng of the MYCN overexpressing pcDNA3.1 plasmid or empty pcDNA3.1 plasmid, and 3 ng of the *Renilla* Luciferase expressing pRL-SV40 plasmid (Promega) for normalization. For transfection, plasmids were incubated with 3 µl CalFectin (SignaGen laboratories, Rockville, MD, USA) in Opti-MEM (Thermo Fisher Scientific) for 20 min before adding the mix dropwise onto the cells. 48 h post-transfection, cells were passively lysed and processed according to the protocol of the Dual-Luciferase® Reporter Assay System (Promega), besides using only half the recommended volume of detection buffers. Firefly and *Renilla* luciferase activities were sequentially measured using a Tecan Spark plate reader and the ratio of firefly luciferase to *Renilla* luciferase luminescence was calculated. The experiments were repeated independently for three times.

RESULTS

EIF4EBP1 expression is increased in NB and correlates with *MYCN* expression

To assess the clinical significance of *EIF4EBP1* expression, we first examined *EIF4EBP1* mRNA levels in NB tumor tissue samples and normal tissues. We pooled microarray data of four different NB cohorts and retrieved expression data from adrenal tissue used as the corresponding normal tissue (Fig. 1a). This indicated that *EIF4EBP1* expression is significantly elevated in NB compared to adrenal gland ($p < 0.0001$, Fig. 1a). We then determined whether *EIF4EBP1* expression is related to the *MYCN* amplification status. By comparing the level of *EIF4EBP1* in *MYCN*-amplified versus *MYCN*-non-amplified NB samples, we found that *EIF4EBP1* is expressed at higher levels in *MYCN*-amplified compared to *MYCN*-non-amplified NB in the SEQC and Kocak cohorts [43, 44] ($p < 0.0001$, Fig. 1b; $p < 0.0001$, Fig. 1c). This further supports and extends previous observations made in a limited number of NB samples ($n = 20$) showing *EIF4EBP1* overexpression in *MYCN*-amplified versus *MYCN*-non-amplified NB tumors [22]. Since *MYCN* amplification may result in different levels of *MYCN*, we next investigated whether expression levels of *MYCN* and *EIF4EBP1* in NB correlate with each other. Our analyses highlighted a significant coexpression between *MYCN* and *EIF4EBP1* in the SEQC (correlation coefficient [r]=0.564, $p < 0.0001$, Fig. 1d) and Kocak ([r]=0.532, $p < 0.0001$, Fig. 1e) cohorts. These findings are in line with the reports that *EIF4EBP1* is a potential MYCN target gene in NB [41, 42]. We also assessed whether the expression of *EIF4EBP1* is determined by NB stages or risk groups, and found that *EIF4EBP1* levels are increased according to NB tumor aggressiveness in two cohorts (Fig. 1f, g). In particular, *EIF4EBP1* is expressed at higher levels in stage 4 NB tumors as compared to stage 1 and stage 2 tumors (stage 4 versus stage 1, $p < 0.0001$, Fig. 1f; $p < 0.0001$ Fig. 1g). Interestingly, samples from stage 4S NB showed significantly lower *EIF4EBP1* levels compared to stage 4 tumors (stage 4S versus stage 4, $p < 0.01$, Fig. 1f; $p < 0.001$, Fig. 1g). In support of this finding, we observed that in the SEQC cohort *EIF4EBP1* expression is higher in high-risk compared to low-risk NB, as based on the Children's Oncology Group (COG) classification ($p < 0.0001$, Fig. 1h). Such clinical information was not available in any other publicly available cohorts with mRNA expression data. Taken together, we present evidence that *EIF4EBP1* is commonly overexpressed in NB tumors and that *EIF4EBP1* level is increased in *MYCN*-amplified NB and advanced NB stages.

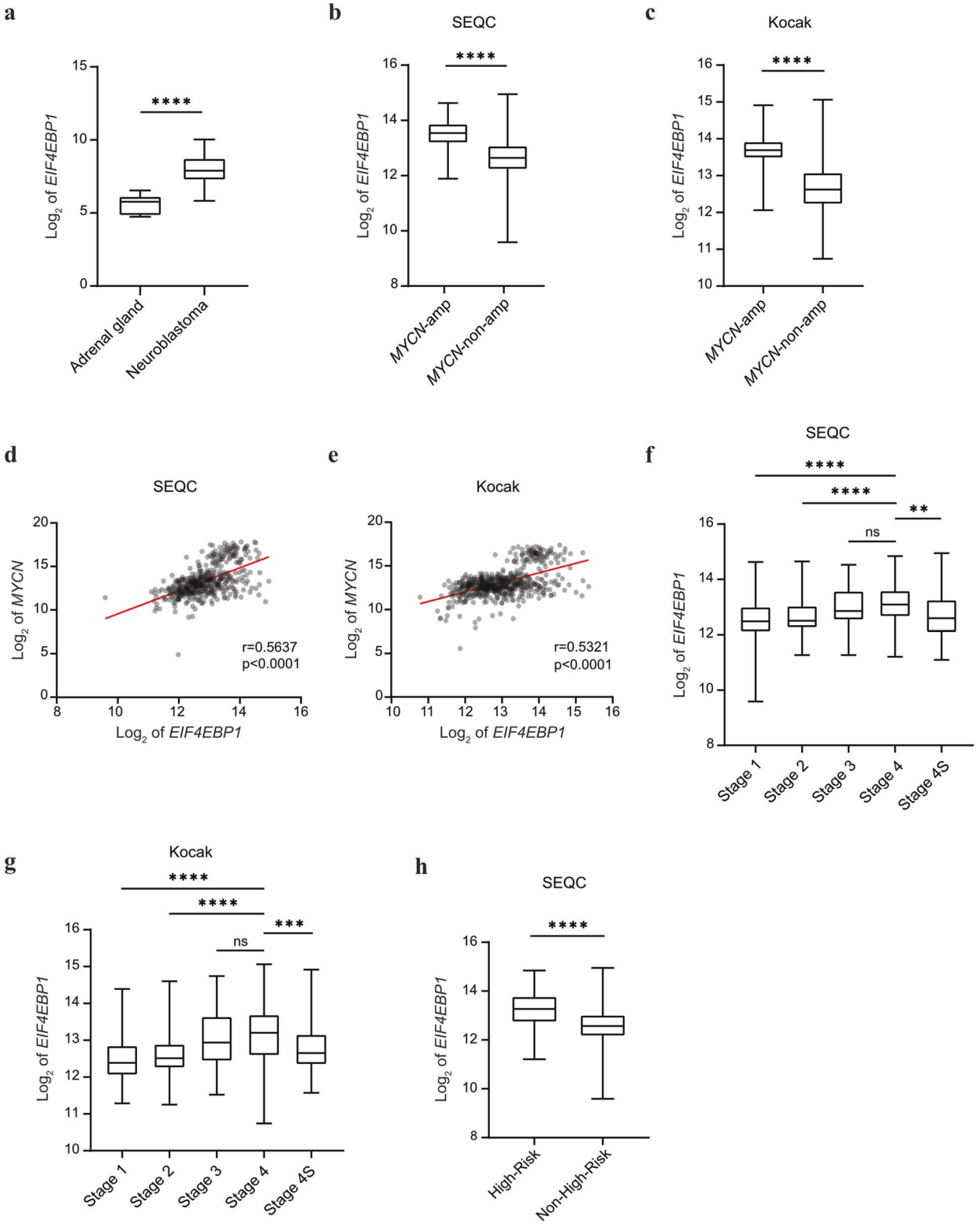

Fig. 1 *EIF4EBP1* mRNA expression is associated with *MYCN* mRNA expression and is increased in more advanced and aggressive NB subsets. a Expression levels of *EIF4EBP1* mRNA in a pool of four different NB cohorts (total $n = 203$), compared to healthy control tissues (adrenal gland, $n = 13$). **b**, **c** Expression levels of *EIF4EBP1* mRNA in *MYCN*-amplified ($n = 92$, SEQC [**b**] and $n = 93$, Kocak [**c**]) compared to *MYCN*-non-amplified ($n = 401$, SEQC [**b**] and $n = 550$, Kocak [**c**]) NB patients of the SEQC (**b**) and Kocak (**c**) cohorts. **d**, **e** Expression levels of *EIF4EBP1* mRNA plotted against expression levels of *MYCN* mRNA in SEQC ($r = 0.5637$, **d**) and Kocak ($r = 0.5321$, **e)** cohorts. **f**, **g** Expression levels of *EIF4EBP1* mRNA per NB stage in SEQC (**f**) and Kocak (**g**) cohorts. **h** Expression levels of *EIF4EBP1* mRNA in high-risk ($n = 176$) compared to non-high-risk ($n = 322$) NB in the SEQC cohort. Data were retrieved from the R2: Genomics Analysis and Visualization Platform. Statistics were determined using Mann–Whitney *U*-test. Exact *p*-values are presented. *$P < 0.05$, **$P < 0.01$, ***$P < 0.001$, ****$P < 0.0001$.

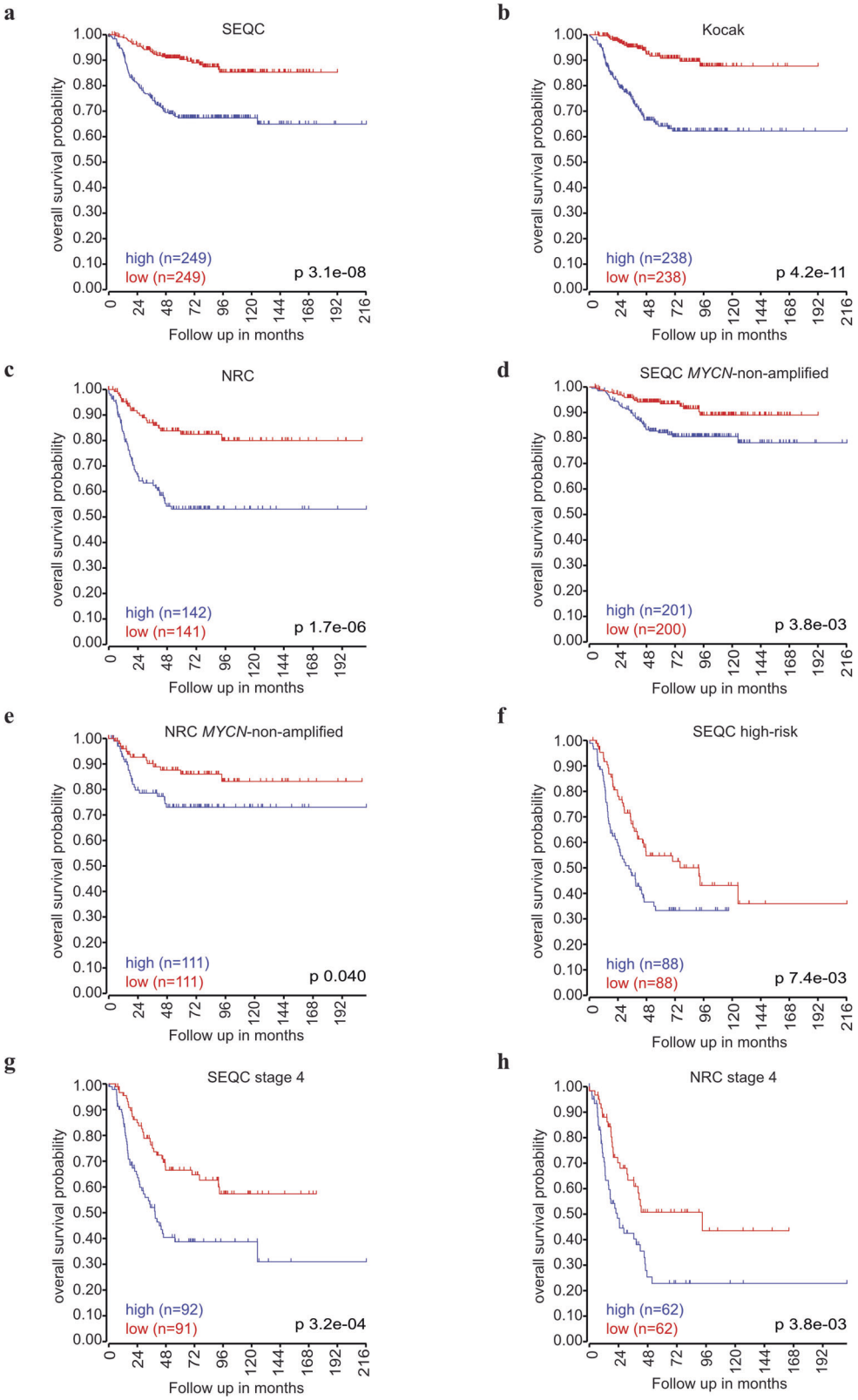

Fig. 2 ***EIF4EBP1*** **mRNA expression correlates with overall survival in NB patients. a**–**c** Kaplan–Meier survival estimates of overall survival of NB patients stratified by their *EIF4EBP1* mRNA expression levels (median cut off) in the SEQC (**a**), Kocak (**b**), and NRC (**c**) cohorts. **d**–**h** Kaplan–Meier survival estimates of overall survival of patients with *MYCN*-non-amplified NB (**d**, **e**), high-risk NB (**f**), or stage 4 NB (**g**, **h**) stratified by their *EIF4EBP1* mRNA expression levels in the indicated NB cohorts. Significance was determined by log-rank test. Data were obtained from the R2: Genomics Analysis and Visualization Platform.

Table 1. Multivariate analysis for overall survival of NB patients in the SEQC cohort.

Variables	HR	95.0% CI	*p* value
MYCN amplification	22.373	8.89–56.306	0
High *EIF4EBP1* mRNA expression	2.16	1.255–3.717	0.005
MYCN amplification*high *EIF4EBP1* mRNA expression	0.222	0.08–0.614	0.004
Stage 4	17.618	6.694–46.366	0
High *EIF4EBP1* mRNA expression	5.457	2.026–14.697	0.001
Stage 4*high *EIF4EBP1* mRNA expression	0.292	0.097–0.879	0.029
Age at diagnosis	33.018	7.835–139.139	0
High *EIF4EBP1* mRNA expression	12.204	2.832–52.598	0.001
Age at diagnosis*high *EIF4EBP1* mRNA expression	0.16	0.035–0.74	0.019

Table 2. Multivariate analysis for overall survival of NB patients in the NRC cohort.

Variables	HR	95.0% CI	*p* value
MYCN amplification	4.967	1.118–22.066	0.035
High *EIF4EBP1* mRNA expression	3.031	1.543–5.954	0.001
MYCN amplification*high *EIF4EBP1* mRNA expression	0.656	0.135–3.181	0.601
Stage 4	15.050	4.239–53.432	0.018
High *EIF4EBP1* mRNA expression	5.144	1.330–19.895	0
Stage 4*high *EIF4EBP1* mRNA expression	0.36	0.081–1.598	0.179
Age at diagnosis	0.27	0.036–2.056	0
High *EIF4EBP1* mRNA expression	0.364	0.048–2.772	0.002
Age at diagnosis*high *EIF4EBP1* mRNA expression	55.427	3.258–942.88	0.005

EIF4EBP1 expression is a factor of poor prognosis in NB

Since we found *EIF4EBP1* mRNA levels to be elevated in aggressive NB subsets, we examined whether *EIF4EBP1* expression is linked to prognosis in NB patients. Kaplan-Meier estimates univocally showed that high *EIF4EBP1* levels (using median expression level as cut off) were significantly associated with reduced overall and event-free survival in three independent cohorts, namely SEQC, Kocak, and NRC cohorts [45] ($p = 3.1e-08$, Fig. 2a; $p = 4.2e-11$, Fig. 2b; $p = 1.7e-06$, Fig. 2c, and supplementary Fig. 1a–c). To test dependence of *EIF4EBP1* expression as prognostic factor on established factors of poor prognosis, we performed multivariate analysis to determine the statistical interaction between high *EIF4EBP1* expression and *MYCN* amplification status, tumor stage or age at diagnosis. This indicated that *MYCN* amplification status, tumor stage and age at diagnosis each influenced the prognostic value of high *EIF4EBP1* expression in the SEQC and NRC cohorts (Tables 1 and 2). Therefore, high *EIF4EBP1* expression is not an independent factor of poor prognosis in NB. However, we uncovered that *EIF4EBP1* expression can predict overall survival in clinically relevant NB subsets, including more advanced and aggressive NB subgroups. Indeed, our analyses highlighted that high *EIF4EBP1* expression significantly predicted reduced overall survival in *MYCN*-non-amplified patients of the SEQC and NRC cohorts ($p = 3.8e-03$, Fig. 2d; $p = 0.04$, Fig. 2e), while it was

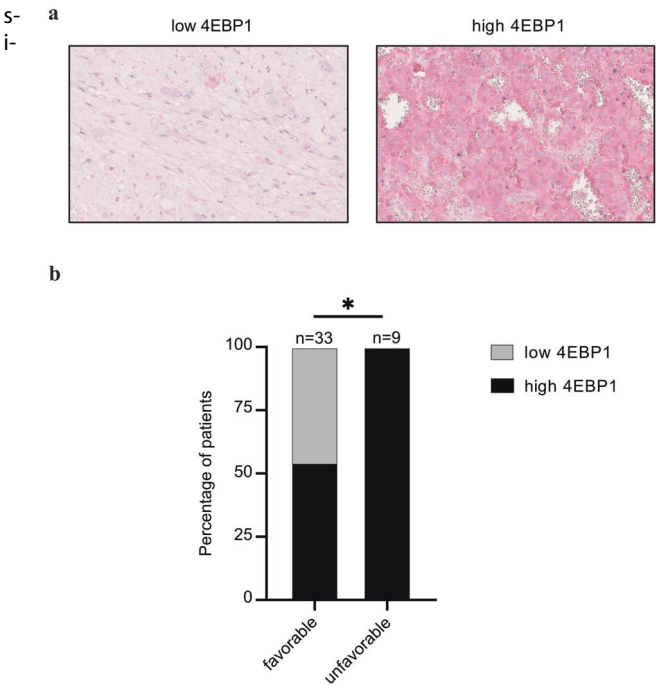

Fig. 3 4EBP1 protein expression is associated with histological subtype of NB. a Representative images at 40X magnification of low (left panel) and high (right panel) 4EBP1 immunohistochemical staining levels of selected NB samples represented on the NB TMAs. **b** Distribution of NB cases showing low (IRS 0–6) versus high (IRS 7–12) 4EBP1 protein expression in prognostically favorable versus unfavorable histological subtypes according to International Neuroblastoma Pathology Classification (INPC). Fisher's exact test was used to calculate significance. *$P < 0.05$.

gnificant for event-free survival only in the SEQC cohort (supplementary Fig. 1d, e). On the other hand, Kaplan–Meier survival estimates in high-risk NB patients (SEQC cohort) revealed that high *EIF4EBP1* levels were correlated with poor overall survival ($p = 7.4e-03$, Fig. 2f), as well as with reduced event-free survival (supplementary Fig. 1f), suggesting that *EIF4EBP1* expression can stratify patients within the most aggressive NB subset. We additionally analyzed the prognostic value of *EIF4EBP1* expression in stage 4 NB patients. We found high *EIF4EBP1* expression to significantly predict decreased overall and event-free survival of stage 4 patients in two independent cohorts (SEQC and NRC cohorts) ($p = 3.2e-04$, Fig. 2g; $p = 3.8e-03$, Fig. 2h and supplementary Fig. 1g, h). This highlights that *EIF4EBP1* expression robustly stratifies patients within the advanced NB subgroups. Altogether, our analyses support that *EIF4EBP1* expression is a factor of poor prognosis in all NB, as well as in high-risk and stage 4 NB.

High 4EBP1 protein expression is associated with prognostically unfavorable histology of NB

To independently confirm the prognostic value of *EIF4EBP1*/4EBP1 in NB and to determine the biomarker potential of 4EBP1 protein expression in NB, we immunohistochemically analyzed NB TMAs consisting of 69 patient samples. Staining of the TMAs with a 4EBP1-specific antibody revealed a cytoplasmic staining (Fig. 3a), consistent with the expected cellular localization of 4EBP1 [46]. We semi-quantitatively evaluated 4EBP1 staining intensity and correlated 4EBP1 immunoreactivity with the NB histological subtypes according to the International Neuroblastoma Pathology Classification (INPC), which distinguishes patients with favorable or unfavorable histology based on grade of neuroblastic differentiation and mitosis-karyorrhexis index. We found that tumors with unfavorable histology more frequently exhibited a high 4EBP1 staining score (IRS 7–12) as compared to tumors with favorable histology (Fig. 3b),

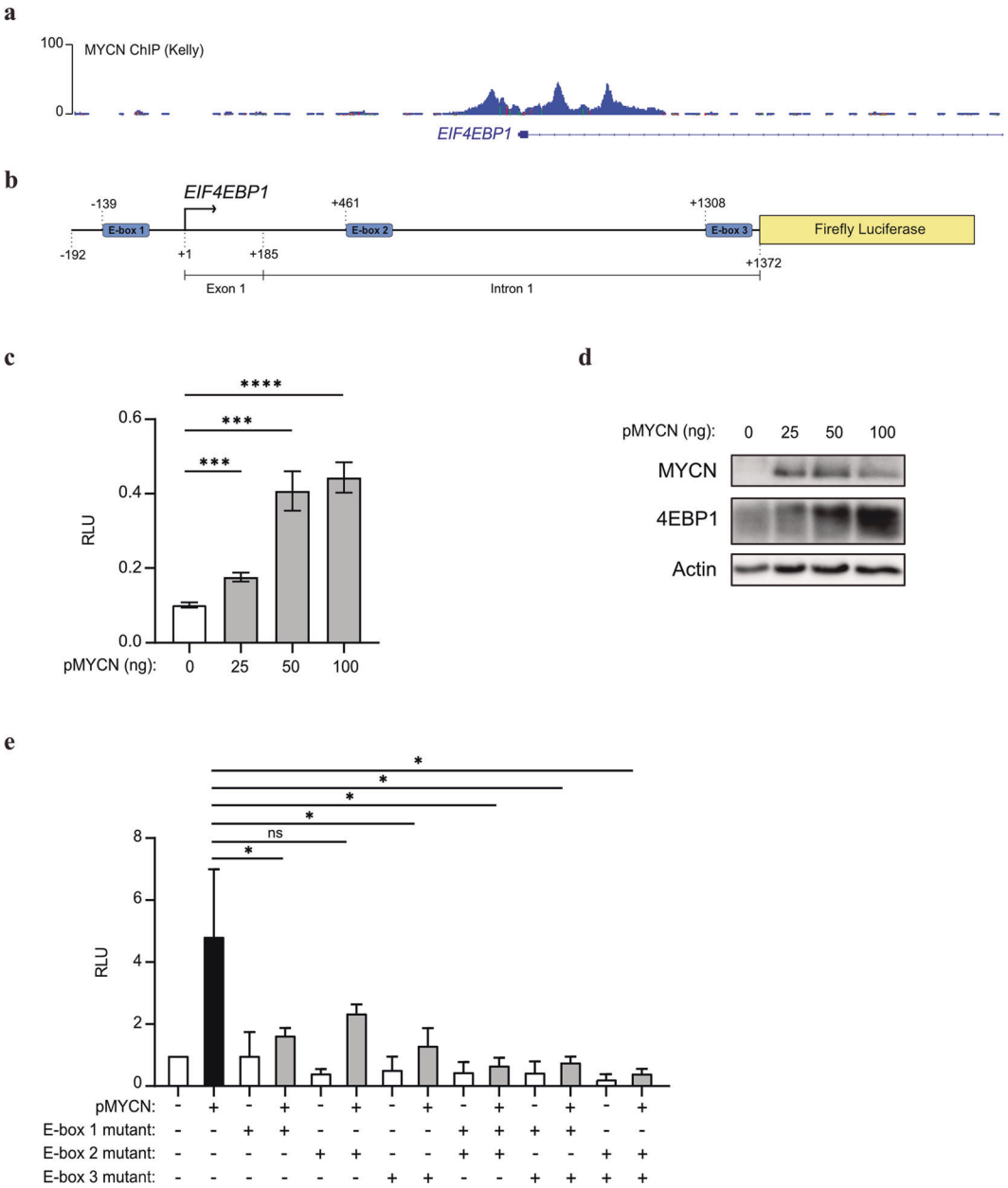

Fig. 4 *EIF4EBP1* promoter activity is regulated by MYCN. a ChIP peaks of MYCN in the *EIF4EBP1* promoter region in Kelly NB cell line. **b** Scheme of the *EIF4EBP1* promoter reporter highlighting the three E-boxes corresponding to MYCN binding sites. **c** HEK-293-T cells were transfected with the wildtype *EIF4EBP1* promoter firefly luciferase construct and with the indicated amounts of MYCN expressing plasmid (pMYCN). A *Renilla* Luciferase vector was used as an internal control. **d** MYCN and 4EBP1 protein expression were monitored in cell lysates from **c** by immunoblot analyses using the indicated antibodies. **e** HEK-293-T were transfected with wildtype or different E-box mutants *EIF4EBP1* promoter firefly luciferase constructs with or without a MYCN expressing plasmid (pMYCN). A *Renilla* Luciferase vector was used as an internal control. Statistics were determined using Student's *t* test or Mann–Whitney *U*-test. Exact *p*-values are presented. **P* < 0.05, ***P* < 0.01, ****P* < 0.001, *****P* < 0.0001.

indicating that high 4EBP1 protein expression is associated with more aggressive NB subsets.

EIF4EBP1 promoter activity and transcription is controlled by MYCN

To delineate how elevated *EIF4EBP1* expression is mechanistically connected to *MYCN* amplification and overexpression in NB, we investigated the transcriptional regulation of *EIF4EBP1* by MYCN. A previous report detected the presence of MYCN on *EIF4EBP1* promoter by ChIP-seq in BE(2)-C, a *MYCN*-amplified NB cell line [41, 42]. We validated and further extended this finding by analyzing ChIP-seq data available from an additional *MYCN*-amplified NB cell line, Kelly. This revealed that MYCN binds the endogenous *EIF4EBP1* promoter region (which encompasses exon 1 and a part of intron 1) at three distinct positions, indicating three potential MYCN binding sites (Fig. 4a). In silico analysis of the promoter region sequence confirmed the presence of structural E-boxes at the three occupied locations (Fig. 4b). To evaluate the impact of MYCN on the regulation of *EIF4EBP1* promoter activity, we designed a luciferase-based gene reporter assay by cloning the *EIF4EBP1* promoter region (−192 to +1372) in front of a firefly luciferase gene (Fig. 4b). The activity of the wildtype *EIF4EBP1* promoter was dose-dependently increased upon forced expression of MYCN in

HEK-293-T cells (Fig. 4c), which was accompanied by an upregulation of endogenous 4EBP1 protein level (Fig. 4d). To investigate which E-boxes are necessary for the transcriptional activation of the *EIF4EBP1* promoter by MYCN, either a single or a combination of two of the three potential binding sites were mutated. Mutation of either of the three binding sites alone was sufficient to significantly reduce MYCN-induced promoter activity (Fig. 4e). Any combinations of two mutated binding sites further reduced promoter activity driven by MYCN overexpression (Fig. 4e), suggesting that two binding sites, without a specific preference of one over another, are needed for full induction of *EIF4EBP1* promoter activity by MYCN. We next intended to confirm whether MYCN directly regulates *EIF4EBP1* transcription in NB cell lines. To do so, we chose two *MYCN*-amplified NB cell lines, IMR-32 and Kelly, in which we knocked down MYCN expression by siRNA and examined the impact on *EIF4EBP1* mRNA levels by qPCR. The depletion of *MYCN* caused a significant reduction of *EIF4EBP1* transcript levels in both cell lines (Fig. 5a, b). To further support these observations, we assessed the impact of forced MYCN expression on *EIF4EBP1* transcript and protein levels by using SHEP-TR-MYCN cells, which are *MYCN*-non-amplified NB cells engineered to express exogenous MYCN with a tetracycline inducible system [19]. Doxycycline treatment markedly increased *EIF4EBP1* mRNA level over time (Fig. 5c), in parallel with progressive upregulation of MYCN expression (Fig. 5d). This was accompanied by a net increase in the 4EBP1 protein level (Fig. 5d), supporting that MYCN positively controls *EIF4EBP1* mRNA and protein expression in NB cells. To determine whether MYCN regulation of *EIF4EBP1* has relevance during NB differentiation, we analyzed expression data of *MYCN*-non-amplified SH-SY5Y cells treated with RA. This indicated that both *MYCN* and *EIF4EBP1* expression are decreased over time upon treatment, and that levels of both genes are correlated during NB differentiation (Fig. 5e–g). Finally, analyses of expression data from a transgenic mouse model of MYCN-driven NB (TH-MYCN; [47]) revealed that *EIF4EBP1* expression is upregulated in NB tumors as compared to the corresponding normal tissue, i.e. the ganglia (Fig. 5h). Taken together, our data provide further evidence that *EIF4EBP1* is a transcriptional target of MYCN, potentially providing a mechanistic basis for the observed overexpression of *EIF4EBP1* in *MYCN*-amplified NB patients.

DISCUSSION

MYCN-amplification is accountable for aggressive NB subsets as it has been associated with increased risk of relapse and reduced overall survival of patients [13]. Since MYCN is considered "undruggable", there is a demand for identifying targetable downstream effectors of MYCN [20, 21]. In addition, since NB is a clinically heterogenous disease, ranging from spontaneous regression to progression despite aggressive therapies, novel markers that improve patient risk stratification and hence allow for optimal treatment allocation are warranted [4, 48, 49]. Here, we report that *EIF4EBP1* expression levels are significantly elevated in NB compared to corresponding non-tumor tissues and positively correlate with both *MYCN* expression and *MYCN* amplification status in at least two independent NB patient cohorts. Furthermore, using three independent NB cohorts, we report that high *EIF4EBP1* expression is a strong predictor of poor overall and event-free survival across all NB patients. This was not independent of *MYCN* amplification status, tumor stage or age at diagnosis, which can be explained in part by the regulation of *EIF4EBP1* promoter by MYCN which we characterized. However, *EIF4EBP1* expression can predict prognosis within distinct patient groups like the *MYCN*-non-amplified patients subset, for which few biomarkers have been identified. Moreover, we observed that high *EIF4EBP1* expression was associated with poor prognosis in the group of patients with aggressive stage 4 NB. Of note, less than a third of stage 4 patients carry a *MYCN* amplification. Thus, it may be worth considering that, in addition to *MYCN* amplification status, levels of *EIF4EBP1* expression could help identifying patients carrying clinically more aggressive tumors within the stage 4 NB patients group. *EIF4EBP1* expression was also linked to worse outcome among high-risk NB patients. Given that *MYCN* amplification is not able of predicting outcome within high-risk NB patients [50], it appears that *EIF4EBP1* expression has a prognostic power beyond *MYCN* amplification in this patient subset. Thus, *EIF4EBP1* expression may represent a promising biomarker for prognostic stratification of high-risk NB patients, in addition to the recently reported genetic alterations in the RAS and p53 pathways [12]. This is further supported by the association we observed between high 4EBP1 protein expression and unfavorable NB histological subtype. Together, our findings highlight a previously underappreciated prognostic factor, i.e., *EIF4EBP1*/4EBP1, which may help refining risk stratification of NB patients, including *MYCN*-non-amplified, stage 4 and high-risk patients, and could potentially assist in tailoring more personalized treatment options. Beyond NB, *EIF4EBP1* expression was reported to be a factor of poor prognosis in breast and liver cancers [30, 33], as well as in all TCGA tumor types combined [29]. While our data indicate that *EIF4EBP1* expression has prognostic power in pediatric cancer, together this supports that *EIF4EBP1* expression represents a factor of poor prognosis in a large number of different tumor types.

Our study also extends previous knowledge by providing further experimental evidence to explain the association between *EIF4EBP1* and *MYCN* expression in NB and the overexpression of *EIF4EBP1* in *MYCN*-amplified NB. Our data revealed that MYCN induces transcription of *EIF4EBP1* by regulating its promoter through multiple binding sites, which was originally suggested by detection of MYCN binding to the *EIF4EBP1* promoter by ChIP analysis [41, 42]. However, whether MYCN could transcriptionally regulate the *EIF4EBP1* promoter was still elusive. We demonstrate that MYCN activates the *EIF4EBP1* promoter through binding at three distinct E-boxes, which in turn leads to transcriptional increase of *EIF4EBP1* even with low to medium MYCN expression, suggesting a threshold for MYCN level. Together with the previous ChIP analysis, this supports that *EIF4EBP1* is a direct target gene of MYCN in NB cells. These findings are in line with previous studies reporting that MYC controls *EIF4EBP1* by binding its endogenous promoter in colorectal and prostate cancer cells [36, 37], as demonstrated by ChIP, highlighting a general regulation of *EIF4EBP1* by MYC family members in cancer cells.

Expression levels of *EIF4EBP1* appear not only elevated in *MYCN*-amplified versus *MYCN*-non-amplified NB but are also upregulated in *MYCN*-non-amplified tumors relative to control tissue. It might be speculated that in *MYCN*-non-amplified NB, *EIF4EBP1* expression may be regulated by transcription factors other than MYCN. In particular, ATF4, which is critical for the metabolic response of NB cells to glutamine starvation [51, 52], has been shown to control *EIF4EBP1* promoter and transcription in pancreatic beta cells [39]. This transcription factor is highly expressed in NB, and in particular in advanced stage 4 [52]. In addition, another transcription factor that is commonly overexpressed in NB is OCT4 [53]. Of note, this transcription factor has been identified by ChIP-seq to bind the promoter region of *EIF4EBP1* in human embryonic stem cells [54, 55], thus OCT4 may also activate *EIF4EBP1* transcription in NB cells. Together, these data suggest potential mechanisms underlying the MYCN independent regulation of *EIF4EBP1* expression in *MYCN*-non-amplified NB patients.

Given the prognostic significance of *EIF4EBP1*/4EBP1 in NB, it is possible that 4EBP1 confers advantages to NB tumor growth or tumor cell survival. As evidenced by the presence of necrotic areas flanked by HIF-1α positive staining [56], NB experience metabolic stress, corresponding to nutrient deprivation and hypoxia, as a consequence of abnormal and immature vascularization [57, 58].

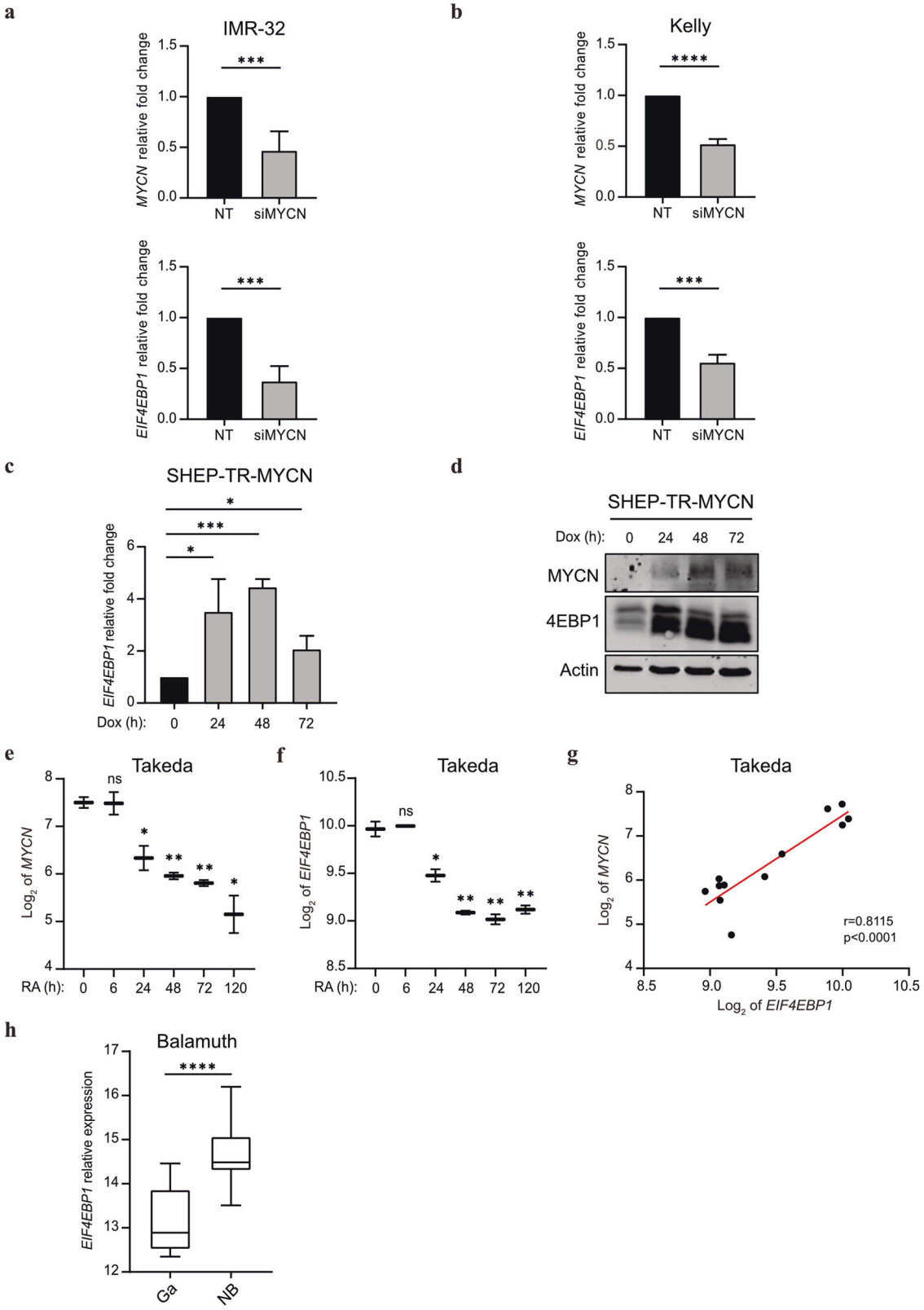

One important mechanism for cancer cells to adapt to metabolic stress is through reprogramming of mRNA translation [59]. As a major regulator of mRNA translation, 4EBP1 may aid NB cells to cope with hypoxia and nutrient deprivation. This is supported by the report that 4EBP1 promotes survival of breast tumors under hypoxia by stimulating the synthesis of pro-angiogenic factors, like HIF-1α and VEGF, to facilitate tumor angiogenesis in vivo [28]. In addition, the control of mRNA translation was shown to be critical to prevent the deleterious effects of MYCN and MYC overexpression, as we and others previously reported [37]. In fact,

Fig. 5 *EIF4EBP1* expression is regulated by MYCN in NB. a, **b** Relative *MYCN* and *EIF4EBP1* mRNA levels upon siRNA-mediated knockdown of *MYCN* in the *MYCN*-amplified IMR-32 (**a**) and Kelly (**b**) cell lines, as measured by qRT-PCR. **c**, **d** SHEP-TR-MYCN cells were treated with doxycycline (1 µg/ml) for the indicated times; *EIF4EBP1* mRNA levels were determined by qRT-PCR (**c**) and levels of MYCN and 4EBP1 proteins were monitored by immunoblot using the indicated antibodies (**d**). The different 4EBP1 bands correspond to different phosphorylated forms of 4EBP1. **e**, **f** Expression levels of *MYCN* (**e**) or *EIF4EBP1* (**f**) mRNA in SH-SY5Y cells treated with RA for the indicated times (Takeda's dataset, $n = 2$ for each time point; [60]). Statistics were calculated for each time point compared to the control 0 h time point. **g** Expression levels of *EIF4EBP1* mRNA plotted against expression levels of *MYCN* mRNA in SH-SY5Y cells treated with RA (Takeda's dataset, $n = 2$ for each time point; [60]). **h** Relative *EIF4EBP1* mRNA expression in healthy control tissues (ganglia, $n = 9$) and NB tumors ($n = 26$) of a TH-MYCN transgenic mouse model of NB (Balamuth's dataset; [47]). Data were retrieved from the R2: Genomics Analysis and Visualization Platform. Statistics were determined using Student's *t* test or Mann–Whitney *U*-test. Exact *p*-values are presented. $^{*}P < 0.05$, $^{**}P < 0.01$, $^{***}P < 0.001$, $^{****}P < 0.0001$.

4EBP1, by reducing overall protein synthesis, was reported to prevent cell death induced upon MYC overexpression, likely by blunting accumulation of misfolded proteins and proteotoxic ER stress [37]. It is possible that in a similar manner 4EBP1 contributes to inhibit cell death induced by MYCN overexpression in *MYCN*-amplified NB.

In summary, the findings reported here indicate that *EIF4EBP1* is a direct target gene of MYCN in NB, explaining the observed high expression of *EIF4EBP1* in NB, and that *EIF4EBP1* mRNA and protein expression have prognostic values in NB patients, especially for stratifying high-risk NB patients.

DATA AVAILABILITY

The data that support the findings of this study are available from the corresponding author upon reasonable request.

REFERENCES

1. Maris JM, Hogarty MD, Bagatell R, Cohn SL. Neuroblastoma. Lancet. 2007;369:2106–20. https://doi.org/10.1016/S0140-6736(07)60983-0
2. van Arendonk KJ, Chung DH. Neuroblastoma: tumor biology and its implications for staging and treatment. Children (Basel) 2019;6. https://doi.org/10.3390/children6010012
3. Tolbert VP, Matthay KK. Neuroblastoma: clinical and biological approach to risk stratification and treatment. Cell Tissue Res. 2018;372:195–209. https://doi.org/10.1007/s00441-018-2821-2
4. Maris JM. The biologic basis for neuroblastoma heterogeneity and risk stratification. Curr Opin Pediatrics. 2005;17:7–13. https://doi.org/10.1097/01.mop.0000150631.60571.89
5. London WB, Castel V, Monclair T, Ambros PF, Pearson ADJ, Cohn SL, et al. Clinical and biologic features predictive of survival after relapse of neuroblastoma: a report from the International Neuroblastoma Risk Group project. J Clin Oncol. 2011;29:3286–92. https://doi.org/10.1200/JCO.2010.34.3392
6. Pinto NR, Applebaum MA, Volchenboum SL, Matthay KK, London WB, Ambros PF, et al. Advances in risk classification and treatment strategies for neuroblastoma. J Clin Oncol. 2015;33:3008–17. https://doi.org/10.1200/JCO.2014.59.4648
7. Simon T, Berthold F, Borkhardt A, Kremens B, Carolis B, de, Hero B. Treatment and outcomes of patients with relapsed, high-risk neuroblastoma: results of German trials. Pediatr Blood Cancer. 2011;56:578–83. https://doi.org/10.1002/pbc.22693
8. Chen Y, Takita J, Choi YL, Kato M, Ohira M, Sanada M, et al. Oncogenic mutations of ALK kinase in neuroblastoma. Nature. 2008;455:971–4. https://doi.org/10.1038/nature07399
9. Mossé YP, Laudenslager M, Longo L, Cole KA, Wood A, Attiyeh EF, et al. Identification of ALK as a major familial neuroblastoma predisposition gene. Nature. 2008;455:930–5. https://doi.org/10.1038/nature07261
10. Janoueix-Lerosey I, Lequin D, Brugières L, Ribeiro A, Pontual L, de, Combaret V, et al. Somatic and germline activating mutations of the ALK kinase receptor in neuroblastoma. Nature. 2008;455:967–70. https://doi.org/10.1038/nature07398
11. Amelio I, Bertolo R, Bove P, Candi E, Chiocchi M, Cipriani C, et al. Cancer predictive studies. Biol Direct. 2020;15:18. https://doi.org/10.1186/s13062-020-00274-3
12. Ackermann S, Cartolano M, Hero B, Welte A, Kahlert Y, Roderwieser A, et al. A mechanistic classification of clinical phenotypes in neuroblastoma. Science. 2018;362:1165–70. https://doi.org/10.1126/science.aat6768
13. Huang M, Weiss WA. Neuroblastoma and MYCN. Cold Spring Harb Perspect Med. 2013;3:a014415. https://doi.org/10.1101/cshperspect.a014415
14. Zeid R, Lawlor MA, Poon E, Reyes JM, Fulciniti M, Lopez MA, et al. Enhancer invasion shapes MYCN-dependent transcriptional amplification in neuroblastoma. Nat Genet. 2018;50:515–23. https://doi.org/10.1038/s41588-018-0044-9
15. Liu R, Shi P, Wang Z, Yuan C, Cui H. Molecular mechanisms of MYCN dysregulation in cancers. Front Oncol. 2020;10:625332. https://doi.org/10.3389/fonc.2020.625332
16. Weiss WA, Aldape K, Mohapatra G, Feuerstein BG, Bishop JM. Targeted expression of MYCN causes neuroblastoma in transgenic mice. EMBO J. 1997;16:2985–95. https://doi.org/10.1093/emboj/16.11.2985
17. Oliynyk G, Ruiz-Pérez MV, Sainero-Alcolado L, Dzieran J, Zirath H, Gallart-Ayala H, et al. MYCN-enhanced oxidative and glycolytic metabolism reveals vulnerabilities for targeting neuroblastoma. iScience. 2019;21:188–204. https://doi.org/10.1016/j.isci.2019.10.020
18. Boon K, Caron HN, van Asperen R, Valentijn L, Hermus MC, van Sluis P, et al. N-myc enhances the expression of a large set of genes functioning in ribosome biogenesis and protein synthesis. EMBO J. 2001;20:1383–93. https://doi.org/10.1093/emboj/20.6.1383
19. Tjaden B, Baum K, Marquardt V, Simon M, Trajkovic-Arsic M, Kouril T, et al. N-Myc-induced metabolic rewiring creates novel therapeutic vulnerabilities in neuroblastoma. Sci Rep. 2020;10:7157. https://doi.org/10.1038/s41598-020-64040-1
20. Bell E, Chen L, Liu T, Marshall GM, Lunec J, Tweddle DA. MYCN oncoprotein targets and their therapeutic potential. Cancer Lett. 2010;293:144–57. https://doi.org/10.1016/j.canlet.2010.01.015
21. Wolpaw AJ, Bayliss R, Büchel G, Dang CV, Eilers M, Gustafson WC, et al. Drugging the "undruggable" MYCN oncogenic transcription factor: overcoming previous obstacles to impact childhood cancers. Cancer Res. 2021;81:1627–32. https://doi.org/10.1158/0008-5472.CAN-20-3108
22. Schramm A, Köster J, Marschall T, Martin M, Schwermer M, Fielitz K, et al. Next-generation RNA sequencing reveals differential expression of MYCN target genes and suggests the mTOR pathway as a promising therapy target in MYCN-amplified neuroblastoma. Int. J. Cancer. 2013;132:E106–15. https://doi.org/10.1002/ijc.27787
23. Musa J, Orth MF, Dallmayer M, Baldauf M, Pardo C, Rotblat B, et al. Eukaryotic initiation factor 4E-binding protein 1 (4E-BP1): a master regulator of mRNA translation involved in tumorigenesis. Oncogene. 2016;35:4675–88. https://doi.org/10.1038/onc.2015.515
24. Morita M, Gravel S-P, Chénard V, Sikström K, Zheng L, Alain T, et al. mTORC1 controls mitochondrial activity and biogenesis through 4E-BP-dependent translational regulation. Cell Metab. 2013;18:698–711. https://doi.org/10.1016/j.cmet.2013.10.001
25. Dowling RJO, Topisirovic I, Alain T, Bidinosti M, Fonseca BD, Petroulakis E, et al. mTORC1-mediated cell proliferation, but not cell growth, controlled by the 4E-BPs. Science. 2010;328:1172–6. https://doi.org/10.1126/science.1187532
26. Wang Z, Feng X, Molinolo AA, Martin D, Vitale-Cross L, Nohata N, et al. 4E-BP1 is a tumor suppressor protein reactivated by mTOR inhibition in head and neck cancer. Cancer Res. 2019;79:1438–50. https://doi.org/10.1158/0008-5472.CAN-18-1220
27. Ding M, van der Kwast TH, Vellanki RN, Foltz WD, McKee TD, Sonenberg N, et al. The mTOR targets 4E-BP1/2 restrain tumor growth and promote hypoxia tolerance in PTEN-driven prostate cancer. Mol Cancer Res. 2018;16:682–95. https://doi.org/10.1158/1541-7786.MCR-17-0696
28. Braunstein S, Karpisheva K, Pola C, Goldberg J, Hochman T, Yee H, et al. A hypoxia-controlled cap-dependent to cap-independent translation switch in breast cancer. Mol Cell. 2007;28:501–12. https://doi.org/10.1016/j.molcel.2007.10.019
29. Wu S & Wagner G. Deep computational analysis of human cancer and non-cancer tissues details dysregulation of eIF4F components and their interactions in human cancers. *bioRxiv* 2020. https://doi.org/10.1101/2020.10.12.336263
30. Karlsson E, Pérez-Tenorio G, Amin R, Bostner J, Skoog L, Fornander T, et al. The mTOR effectors 4EBP1 and S6K2 are frequently coexpressed, and associated with a poor prognosis and endocrine resistance in breast cancer: a retrospective study including patients from the randomised Stockholm tamoxifen trials. Breast Cancer Res. 2013;15:R96. https://doi.org/10.1186/bcr3557
31. Kremer CL, Klein RR, Mendelson J, Browne W, Samadzedeh LK, Vanpatten K, et al. Expression of mTOR signaling pathway markers in prostate cancer progression. Prostate. 2006;66:1203–12. https://doi.org/10.1002/pros.20410

32. Lee M, Kim EJ, Jeon MJ. MicroRNAs 125a and 125b inhibit ovarian cancer cells through post-transcriptional inactivation of EIF4EBP1. Oncotarget. 2016;7:8726–42. https://doi.org/10.18632/oncotarget.6474
33. Cha Y-L, Li P-D, Yuan L-J, Zhang M-Y, Zhang Y-J, Rao H-L, et al. EIF4EBP1 overexpression is associated with poor survival and disease progression in patients with hepatocellular carcinoma. PLoS ONE. 2015;10:e0117493. https://doi.org/10.1371/journal.pone.0117493
34. Fransson S, Abel F, Kogner P, Martinsson T, Ejeskär K. Stage-dependent expression of PI3K/Akt-pathway genes in neuroblastoma. Int J Oncol. 2013;42:609–16. https://doi.org/10.3892/ijo.2012.1732
35. Meng X, Li H, Fang E, Feng J, Zhao X. Comparison of stage 4 and stage 4s neuroblastoma identifies autophagy-related gene and LncRNA signatures associated with prognosis. Front Oncol. 2020;10:1411. https://doi.org/10.3389/fonc.2020.01411
36. Balakumaran BS, Porrello A, Hsu DS, Glover W, Foye A, Leung JY, et al. MYC activity mitigates response to rapamycin in prostate cancer through eukaryotic initiation factor 4E-binding protein 1-mediated inhibition of autophagy. Cancer Res. 2009;69:7803–10. https://doi.org/10.1158/0008-5472.CAN-09-0910
37. Tameire F, Verginadis II, Leli NM, Polte C, Conn CS, Ojha R, et al. ATF4 couples MYC-dependent translational activity to bioenergetic demands during tumour progression. Nat Cell Biol. 2019;21:889–99. https://doi.org/10.1038/s41556-019-0347-9
38. Liu Y, Horn JL, Banda K, Goodman AZ, Lim Y, Jana S et al. The androgen receptor regulates a druggable translational regulon in advanced prostate cancer. Sci Transl Med. 2019;11. https://doi.org/10.1126/scitranslmed.aaw4993
39. Yamaguchi S, Ishihara H, Yamada T, Tamura A, Usui M, Tominaga R, et al. ATF4-mediated induction of 4E-BP1 contributes to pancreatic beta cell survival under endoplasmic reticulum stress. Cell Metab. 2008;7:269–76. https://doi.org/10.1016/j.cmet.2008.01.008
40. Azar R, Lasfargues C, Bousquet C, Pyronnet S. Contribution of HIF-1α in 4E-BP1 gene expression. Mol. Cancer Res. 2013;11:54–61. https://doi.org/10.1158/1541-7786.MCR-12-0095
41. Cheung CHY, Hsu C-L, Tsuei C-Y, Kuo T-T, Huang C-T, Hsu W-M, et al. Combinatorial targeting of MTHFD2 and PAICS in purine synthesis as a novel therapeutic strategy. Cell Death Dis. 2019;10:786. https://doi.org/10.1038/s41419-019-2033-z
42. Hsu C-L, Chang H-Y, Chang J-Y, Hsu W-M, Huang H-C, Juan H-F. Unveiling MYCN regulatory networks in neuroblastoma via integrative analysis of heterogeneous genomics data. Oncotarget. 2016;7:36293–310. https://doi.org/10.18632/oncotarget.9202
43. SEQC/MAQC consortium. SEQC/MAQC consortium: a comprehensive assessment of RNA-seq accuracy, reproducibility and information. Nat Biotechnol. 2014;32:903–14. https://doi.org/10.1038/nbt.2957
44. Kocak H, Ackermann S, Hero B, Kahlert Y, Oberthuer A, Juraeva D, et al. Hox-C9 activates the intrinsic pathway of apoptosis and is associated with spontaneous regression in neuroblastoma. Cell Death Dis. 2013;4:e586. https://doi.org/10.1038/cddis.2013.84
45. Rajbhandari P, Lopez G, Capdevila C, Salvatori B, Yu J, Rodriguez-Barrueco R, et al. Cross-cohort analysis identifies a TEAD4-MYCN positive feedback loop as the core regulatory element of high-risk neuroblastoma. Cancer Discov. 2018;8:582–99. https://doi.org/10.1158/2159-8290.CD-16-0861
46. Armengol G, Rojo F, Castellví J, Iglesias C, Cuatrecasas M, Pons B, et al. 4E-binding protein 1: a key molecular "funnel factor" in human cancer with clinical implications. Cancer Res. 2007;67:7551–5. https://doi.org/10.1158/0008-5472.CAN-07-0881
47. Balamuth NJ, Wood A, Wang Q, Jagannathan J, Mayes P, Zhang Z, et al. Serial transcriptome analysis and cross-species integration identifies centromere-associated protein E as a novel neuroblastoma target. Cancer Res. 2010;70:2749–58. https://doi.org/10.1158/0008-5472.CAN-09-3844
48. Rugolo F, Bazan NG, Calandria J, Jun B, Raschellà G, Melino G, et al. The expression of ELOVL4, repressed by MYCN, defines neuroblastoma patients with good outcome. Oncogene. 2021;40:5741–51. https://doi.org/10.1038/s41388-021-01959-3
49. Pieraccioli M, Nicolai S, Pitolli C, Agostini M, Antonov A, Malewicz M, et al. ZNF281 inhibits neuronal differentiation and is a prognostic marker for neuroblastoma. Proc. Natl Acad. Sci. USA. 2018;115:7356–61. https://doi.org/10.1073/pnas.1801435115
50. Lee JW, Son MH, Cho HW, Ma YE, Yoo KH, Sung KW, et al. Clinical significance of MYCN amplification in patients with high-risk neuroblastoma. Pediatr Blood Cancer. 2018;65:e27257. https://doi.org/10.1002/pbc.27257
51. Qing G, Li B, Vu A, Skuli N, Walton ZE, Liu X, et al. ATF4 regulates MYC-mediated neuroblastoma cell death upon glutamine deprivation. Cancer Cell. 2012;22:631–44. https://doi.org/10.1016/j.ccr.2012.09.021
52. Ren P, Yue M, Xiao D, Xiu R, Gan L, Liu H, et al. ATF4 and N-Myc coordinate glutamine metabolism in MYCN-amplified neuroblastoma cells through ASCT2 activation. J Pathol. 2015;235:90–100. https://doi.org/10.1002/path.4429
53. Yang S, Zheng J, Ma Y, Zhu H, Xu T, Dong K, et al. Oct4 and Sox2 are overexpressed in human neuroblastoma and inhibited by chemotherapy. Oncol Rep. 2012;28:186–92. https://doi.org/10.3892/or.2012.1765
54. Gifford CA, Ziller MJ, Gu H, Trapnell C, Donaghey J, Tsankov A, et al. Transcriptional and epigenetic dynamics during specification of human embryonic stem cells. Cell. 2013;153:1149–63. https://doi.org/10.1016/j.cell.2013.04.037
55. Čančer M, Hutter S, Holmberg KO, Rosén G, Sundström A, Tailor J, et al. Humanized stem cell models of pediatric medulloblastoma reveal an Oct4/mTOR axis that promotes malignancy. Cell Stem Cell. 2019;25:855–870.e11. https://doi.org/10.1016/j.stem.2019.10.005
56. Påhlman S, Mohlin S. Hypoxia and hypoxia-inducible factors in neuroblastoma. Cell Tissue Res. 2018;372:269–75. https://doi.org/10.1007/s00441-017-2701-1
57. Schaaf MB, Garg AD, Agostinis P. Defining the role of the tumor vasculature in antitumor immunity and immunotherapy. Cell Death Dis. 2018;9:115. https://doi.org/10.1038/s41419-017-0061-0
58. Lugano R, Ramachandran M, Dimberg A. Tumor angiogenesis: causes, consequences, challenges and opportunities. Cell Mol Life Sci. 2020;77:1745–70. https://doi.org/10.1007/s00018-019-03351-7
59. Leprivier G, Rotblat B, Khan D, Jan E, Sorensen PH. Stress-mediated translational control in cancer cells. Biochim. Biophys. Acta. 2015;1849:845–60. https://doi.org/10.1016/j.bbagrm.2014.11.002
60. Nishida Y, Adati N, Ozawa R, Maeda A, Sakaki Y, Takeda T. Identification and classification of genes regulated by phosphatidylinositol 3-kinase- and TRKB-mediated signalling pathways during neuronal differentiation in two subtypes of the human neuroblastoma cell line SH-SY5Y. BMC Res Notes. 2008;1:95. https://doi.org/10.1186/1756-0500-1-95

ACKNOWLEDGEMENTS

We would like to thank Dr. Bastian Malzkorn (Institute of Neuropathology, Heinrich Heine University Düsseldorf) for helpful discussions. GL was supported by funding from the Elterninitiative Düsseldorf e.V., the Research Commission of the Medical Faculty of Heinrich Heine University, the Deutsche Forschungsgemeinschaft (Grant LE 3751/2-1), and the German Cancer Aid (Grant 70112624). The laboratory of TGPG is supported by the Barbara und Wilfried Mohr Foundation. BR is supported by the Israel Science Foundation (grant No. 1436/19).

AUTHOR CONTRIBUTIONS

Conception and design: KV and GL. Provision of study material and patients: IE and TK. Financial and administrative support: GR. Data analysis and interpretation: KV, TGPG, AS, and GL. Critical review and discussion: BR, MR, AS, GR, and GL. Experimental support: KV, KS, CF, AK, DP, LH, and MFO. Manuscript writing: KV, GR, and GL. Final approval of the manuscript: all authors.

FUNDING

Open Access funding enabled and organized by Projekt DEAL.

COMPETING INTERESTS

TK received honoraria for Consulting/Advisory by Amgen, AstraZeneca, BMS, Merck KGaA, MSD, Novartis, Pfizer, Roche, for Research Funding by Merck KGaA and Roche; for talks by Merck KGaA, AstraZeneca. The other authors declare no conflict of interest.

ADDITIONAL INFORMATION

Supplementary information The online version contains supplementary material available at https://doi.org/10.1038/s41420-022-00963-0.

Correspondence and requests for materials should be addressed to Gabriel Leprivier.

Reprints and permission information is available at http://www.nature.com/reprints

Publisher's note Springer Nature remains neutral with regard to jurisdictional claims in published maps and institutional affiliations.